PERFORMANCE OF MACHINE AND DEEP LEARNING METHODS IN FORECASTING OF GLOBAL IONOSPHERE MAPS

Erman Şentürk [1*]

[1] Kocaeli University, Department of Geomatics, Turkey

ORCID ID: 0000-0002-0833-7113, erman.senturk@kocaeli.edu.tr

**** Corresponding Author***

Abstract

The ionosphere is an atmosphere layer that causes delay/acceleration effects on electromagnetic signals traveling between space and earth due to the containing number of free electrons. Forecasting the number of free electrons is an important field of study for space weather, communication, and navigation applications. In this study, artificial intelligence (AI) techniques e.g. a machine learning-based method, autoregressive integrated moving average (ARIMA), and a deep learning-based method, long short-term memory (LSTM) network, were utilized in producing predicted Global Ionosphere Maps (GIMs). The vertical Total Electron Content (VTEC) values of the International GNSS Service (IGS)-GIMs between March 1 and March 31, 2020 were trained at all grid points (71x73 grids) and VTEC values on April 1-2 were forecasted with the proposed models. Also, the forecast VTEC values obtained from the 1 and 2 days predicted GIMs (pGIMs) produced by CODE (c1pg, c2pg) and the forecast VTEC values of proposed methods were compared with the observed VTEC values of the final IGS-GIMs (igsg). The results showed that ARIMA predicted VTEC values with lower accuracy than LSTM and c1pg-c2pg. LSTM method has very close prediction accuracy to c1pg-c2pg, but the results of CODE-pGIMs are more consistent with the final IGS-GIMs. Future work aims to achieve better results than pGIMs of IGS analysis centers (CODE, ESA, UPC, IGS combined) by changing the hyperparameters of the LSTM (e.g. increasing the number of hidden layers or iterations, using long-term training data) or using modified versions of LSTM (e.g. Bi-LSTM). In particular, we foresee that the multivariate approach will further improve the results of the proposed methods.

Keywords: *ARIMA, Forecasting, Ionosphere, LSTM, Predicted GIMs, Total Electron Content*

1. Introduction

The ionosphere is an ionized Earth's atmosphere layer due to the solar and cosmic radiation which locates at 80-1000 km above the Earth's surface. The molecules in this layer emit free electrons when exposed to solar radiation. The ionosphere is divided into three different layers as D, E, F1, and F2 according to the thermal and chemical properties of the uncharged gas and ionized components that vary according to height. The lower layers (D and E) of the ionosphere provide radio communication around the world by reflecting low/high-frequency radio signals (VLF, LF, MF, and HF). The upper layers (F1 and especially F2) cause an important source of error in navigation applications due to the delay (code observations) and acceleration (phase observations) effects on the Global Navigation Satellite Systems (GNSS) signals. Therefore, the ionosphere is an essential atmosphere layer for communication and navigation applications, and modeling or forecasting the momentary number of free electrons is an important field of study.

Because GNSS technology provides low-cost, high accuracy, near-real-time, and continuity ionospheric data, it has been used extensively in ionosphere modeling studies in recent decades (Ho et al., 1996; Mannucci et al., 1998; Fedrizzi et al., 2002; Brunini et al., 2004; Hernández-Pajares et al., 2011; Reddybattula et al., 2019). Since the ionospheric effect on electromagnetic signals is frequency-dependent, VTEC values can be calculated by GNSS observations. In addition, the error caused by the ionospheric delay/acceleration effect on the pseudorange can be eliminated in dual-frequency receivers. Although the ionosphere error can be eliminated with dual-frequency

receivers, the high cost of these devices prevents them from being used in practical applications. Here, inexpensive single-frequency receivers are used and the ionospheric delay error is tried to be removed by various ionospheric models such as Klobuchar, NeQuick, GIMs. The most used model for real-time GPS navigation applications is the Klobuchar coefficients (4 alpha and 4 beta coefficients) included in the GPS broadcast ephemeris (brdc) files. However, this model can eliminate only 50% of the ionospheric error (Klobuchar, 1987). Especially in adverse space climate conditions, errors are gradually increasing. Orus-Perez (2019) proposed a TensorFlow-based neural network model to estimate GNSS single frequency ionospheric delay. Recently, new ionospheric global models for long-term forecasting such as the Neustrelitz TEC Model (NTCM) (Jakowski et al. 2011) and the GEMTEC (Ivanov et al. 2011) have been developed based on GIMs.

There are many traditional time series analysis methods to modeling the VTEC time series, but these methods are not adequate to simulation the previous VTEC values and the pattern that is far away from forecasting-initial-point, as any artificial intelligence (AI) algorithms. However, the AI method learns the trend, seasonality, and residuals patterns in the VTEC time series and successfully forecasting VTEC values for a short period. Some AI-based methods were previously utilized to forecast ionospheric parameters (McKinnell and Poole, 2004; Athieno et al., 2017; Sai Gowtam and Tulasi Ram, 2017; Srivani et al., 2019; Kaselimi et al., 2020; li et al., 2020; Ruwali et al., 2020). McKinnell and Poole (2004) trained a neural network (NN) based ionospheric model to reveal the development of the F layer contribution. They indicated that NNs can be utilized to provide solutions to difficult prediction tasks such as the probability of F1 layer existence. Athieno et al. (2017) developed a Neural Network (NN) model to forecast the critical frequency of the F2 layer (foF2) values in the polar cap. The results showed that the NN model performs better than IRI2012 during low solar activity and the equinoxes. Sai Gowtam and Tulasi Ram (2017) developed an ANN-based two-dimensional (2-D) Ionospheric Model (ANNIM) to predict the ionospheric peak parameters, such as NmF2 and hmF2 using FORMOSAT-3/COSMIC data from 2006 to 2015. ANNIM has captured the global-scale ionospheric phenomena such as ionospheric annual anomaly, Weddell Sea Anomaly, and the midlatitude summer nighttime anomaly. Li et al. (2020) utilized the state-of-the-art artificial neural network (ANN) technique optimized by the genetic algorithm for a long-term forecast of the NmF2 and foF2 global distribution. They indicated that ANN models have good capability to specify ionospheric spatial-temporal characteristics both in global and local. Ruwali et al. (2020) compared some deep learning models, long short-term memory, gated recurrent unit, and a hybrid model that consists of LSTM combined with convolution neural network (CNN) to forecast the ionospheric delays for GPS signals. They demonstrated that the LSTM-CNN model performs well according to other methods.

In this study, we produced predicted GIMs (pGIMs) using ARIMA and LSTM methods and compared the daily average (bias) and root mean square (RMS) error values of the differences between our pGIMs, 1-2 days pGIMs by the Center for Orbit Determination in Europe (CODE) (c1pg, c2pg) and final IGS GIMs (igsg). The VTEC data of final IGS GIMs were trained for 31 days (12 data points in one day) from March 1 to March 31, 2020, and forecasted the VTEC values of the subsequent 2 days (April 1-2, 2020) by fitted models with optimal hyperparameters. Here, we used the direct method. In other words, we created the time series at all grid points and analyzed them separately.

2. Data and Methodology

We proposed a machine learning-based method, ARIMA, and a deep learning-based method, LSTM network to produce pGIMs. ARIMA is a time series model based on traditional statistical concepts and integration of two methods: Auto Regression (AR) and Moving Average (MA). LSTM is a type of recurrent neural network (RNN) architecture. While conventional neural network (CNN) is advanced enough to capture and learn the irregularity in a time series and forecasts upcoming value when it is highly correlated with the previous terms, it is not sufficient success in forecasting long time series due to their feedforward structure. The recurrent neural network (RNN)

used to pass previous learning to the adjacent nodes but it has not any memory power to keep nodes that are far away from the current node, and cannot capture long-term dependencies due to vanishing/exploding gradients during backpropagation. LSTM addresses the vanishing/exploding gradient problem and allows learning of long-term dependencies. We split our analysis into three divisions: (1) data collection from GIMs and pre-processing (2) formulation of the models, and (3) implementations.

2.1. Global Ionosphere Maps (GIMs) and predicted GIMs (pGIMs)

The Total Electron Content (TEC) is an ionospheric parameter that describes the free electron content by GNSS observations. The unit of TEC is TECU which equal to 10^{16} electrons/m^2 in a cylinder with a 1-meter radius along the path of the signal traveling in the ionosphere. The magnitude of the ionospheric effect on the electromagnetic signals is related to the STEC (Slant Total Electron Content) values calculated along the oblique path of the signal. Since the slant TEC is dependent on the signal path geometry through the ionosphere, an equivalent vertical value of TEC is calculated that is independent of the elevation of the signal path (Sharma et al., 2012). The ionosphere is generally divided into several layers of varying thickness according to electron density (Hargreaves, 1992). The single-layer model assumes that a thin spherical shell is located at a specified altitude so that the STEC can be converted to the vertical TEC (VTEC). The point where the signal penetrated a thin shell is called Ionospheric Piercing Points (IPPs). While VTEC values can be calculated for a single station, the Regional Ionosphere Maps (RIMs) with surface interpolation and the Global Ionosphere Maps (GIMs) with spherical harmonics are produced from VTEC values at IPPs. In order to produce GIMs, VTEC data collected from over 400 stationary GNSS stations (IGS network) spread over the world are modeled with spherical harmonic series depending on geographical coordinates. GIMs provide worldwide VTEC data with 15-minute to 2-hours temporal resolution and 2.5^0 x 5^0 spatial resolution in latitude and longitude, respectively. IGS Ionosphere Associate Analysis Centers (IAACs) provide three different types of GIMs: rapid (1 day after), final (1-2 weeks after), predicted (1-2 days before) via the Ionosphere Map Exchange Format (IONEX) files. These files are freely available in ftp://cddis.gsfc.nasa.gov/gps/products/ionex/.

Table 1: The predicted GIMs producing by IGS's IAACs (https://cddis.nasa.gov/Data_and_Derived_Products/GNSS/atmospheric_products.html)

IONEX file code	Meaning
c1p	1-day predicted solution (CODE)
c2p	2-day predicted solution (CODE)
e1p	1-day predicted solution (ESA)
e2p	2-day predicted solution (ESA)
ilp	1-day predicted solution (IGS combined)
i2p	2-day predicted solution (IGS combined)
u2p	2 day predicted solution (UPC)

2.2. ARIMA Method

ARIMA models are used to analyze time-series data and forecasting the next values from the past values of the time series and the prediction errors. The method is a combination of two traditional statistical concepts, Auto Regression (AR) and Moving Average (MA). By combining these models, Box and Jenkings (1970) developed the ARIMA method to show the transformations required for the use of models in non-stationary series, to examine the statistical properties of the models extensively, to find a model suitable for the available time-series data, to estimate the parameters of the model and to test the fit of the model. The general usage of the method is arima (p, d, q) where,

- p is the number of autoregressive terms,
- d is the number of nonseasonal differences needed for stationarity,
- q is the number of moving averages.

To apply the ARIMA method, the stationarity test of the time series must first be performed. Here, the Augmented Dickey-Fuller (ADF) conducts to test the stationarity of the data. ADF method tested H_0 (the population is non-stationary) and H_1 (the population is stationary) hypothesis (Pedregosa et al., 2011). The p-value less than 0.05 (5% confidence interval) indicates the strong probability of acceptance of alternative hypothesis (H_1), so ARIMA can be applied to a time series.

Jenkins and Box proposed a method to define the parameters of ARIMA (p and q) using the autocorrelation function (ACF) and the partial autocorrelation function (PACF) of the sample data. The value of the parameter q is determined from the ACF plot and the value of the p parameter from the PACF plot (Fuller, 2009). In the ACF and PACF plots, where the lines intersect the zero value downward, the nearest integer value of the lags determines the parameters' value.

We can formulate ARIMA (p, d, q) as follows:

$$Y_t = \delta + \alpha_1 Y_{t-1} + \alpha_2 Y_{t-2} + \alpha_3 Y_{t-3} + \cdots + \alpha_p Y_{t-p} + \varepsilon_t - \theta_1 \varepsilon_{t-1} - \theta_2 \varepsilon_{t-2} - \theta_3 \varepsilon_{t-3} - \cdots - \theta_q \varepsilon_{t-q} \quad (1)$$

where δ is a constant, Y_t is linear combinations of the previous time-series terms with the coefficients $\alpha_1, \alpha_2, \alpha_3, \ldots, \alpha_p$ and ε_t is a random shock at time t.

2.3. LSTM Method

LSTM is a type of RNN developed to understand long-term dependencies in artificial neural networks, thus obtaining context-aware neural networks. It was proposed in Hochreiter and Schmidhuber (1997) to overcome the problem of vanishing/exploding gradient caused by feedback neural networks models. The special architectures of the LSTM-RNN network (Figure 1) made it possible to keep those learning within the network and forecast based on these learning. LSTM networks have four components: Cell State, Input Gate, Forget Gate, and Output Gate (Figure 1b).

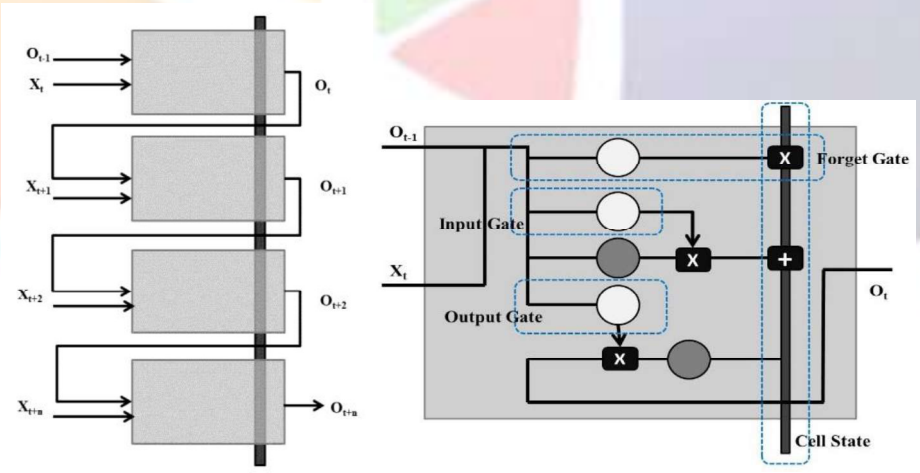

(a) (b)

Figure 1: The architecture of LSTM. (a) the complete connected architecture, (b) one-single-node representation.

Let input is X_t, weight vector $W_t = [w_f, w_i, w_c, w_o]$, bias $b_t = [b_f, b_i, b_c, b_o]$, and output O_t at time t. The first step in LSTM is to decide the information that is not required for the cell state with a sigmoid layer called the forget gate layer.

$$f_t = \sigma(w_f[O_{t-1}, X_t] + b_f) \quad (2)$$

In the next step, which values to update are decided by a sigmoid layer called the input gate layer, and then a tanh layer creates a vector of new candidate values that can be added to the state. Thus, new information is stored in the cell state.

$$i_t = \sigma(w_i[O_{t-1}, X_t] + b_i) \tag{3}$$

$$C_t^{\sim} = tanh(w_c[O_{t-1}, X_t] + b_c) \tag{4}$$

Now, the old cell state, C_{t-1}, multiplied by f_t and added $i_t * C_t^{\sim}$ which indicates the candidate values scaled by updated each state value. This process will update the old cell state into the new cell state.

$$C_t = f_t * C_{t-1} + i_t * C_t^{\sim} \tag{5}$$

Finally, we put the new cell state in tanh (values are normalized between -1 and 1) and, multiplying by the sigmoid gate, so we decide the information to be transferred from the cell state to the output gate.

$$h_t = \sigma(w_O[O_{t-1}, X_t] + b_O) \tag{6}$$

$$O_t = h_t * \tanh(C_t) \tag{7}$$

2.4. Implementations

ARIMA and LSTM models were implemented in the MATLAB R2019b using Econometrics and Deep Learning Toolboxes. Two statistical metrics employed to evaluate the performance of the proposed models; Bias and Root Mean Square (RMS) error.

$$\text{BIAS} = \frac{1}{n}\sum_{i=1}^{n} \text{VTEC}_{\text{Forecast}} - \text{VTEC}_{\text{Observed}} \tag{8}$$

$$\text{RMS} = \sqrt{\frac{1}{n}\sum_{i=1}^{n} (\text{VTEC}_{\text{Forecast}} - \text{VTEC}_{\text{Observed}})^2} \tag{9}$$

3. Results

As mentioned in the previous sections, the forecasting performance of the ARIMA and LSTM methods depends on the stationarity of the VTEC time series. Ionospheric variation has the same daily min-max values with little erratum but this erratum becomes high during any special events e.g. magnetic storms, solar activity. In order to understand the effect of space weather on the variation of the VTEC time series, we first analyzed some space weather conditions. The quiet space weather period is generally decided by threshold values of Dst > -20 nT, F10.7 < 90 sfu. In Figure 2, the Dst, V_{SW}, Kp, and F10.7 space weather indices were demonstrated from March 1 to April 2, 2020. Figures 1a and 1c demonstrate the variations of Dst and Kp magnetic activity indices. These indices indicate quiet magnetic activity during the related time interval. Figures 1b and 1d present the variations of V_{SW} and F10.7 solar activity indices. These indices also were at values representing low solar activity, so the VTEC time series was sufficiently stationary in the period of the VTEC data used for analysis.

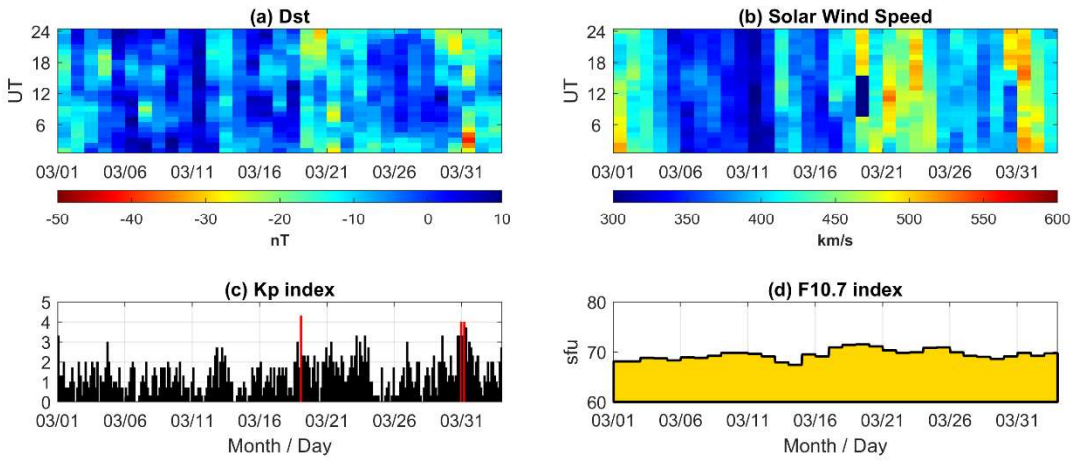

Figure 2: The variation of solar activity (Solar wind speed, F10.7) and geomagnetic storm (Dst, Kp) indices between March 1 and April 2, 2020.

The final IGS GIMs (igsg) and CODE pGIMs (c1pg and c2pg) were used to investigate the performance of the proposed methods. The daily bias and RMS values of the differences between the forecast products (ARIMA, LSTM, and CODE) and final IGS GIMs were used as reference values. The total number of VTEC values for daily GIM products is equal to 67379 (71 × 73 × 13). We trained these data for 31 days from March 1 to March 31, 2020.

Figures 3 show the VTEC maps of forecasting products and the final IGS GIMs on April 1-2, 2020. Also, the daily RMS values of the differences between the forecast products and final IGS GIMs are demonstrated in Figure 4. The daily RMS values shown in Figure 4 indicate that there is better consistency between CODE pGIMs and final IGS GIMs than forecast products of proposed methods.

The daily RMS values generally peaked in the equatorial anomaly region in all models. This result indicated that it is difficult to accurately forecast VTEC values in the equatorial ionization anomaly (EIA) region due to the complex dynamics of the ionosphere in this region.

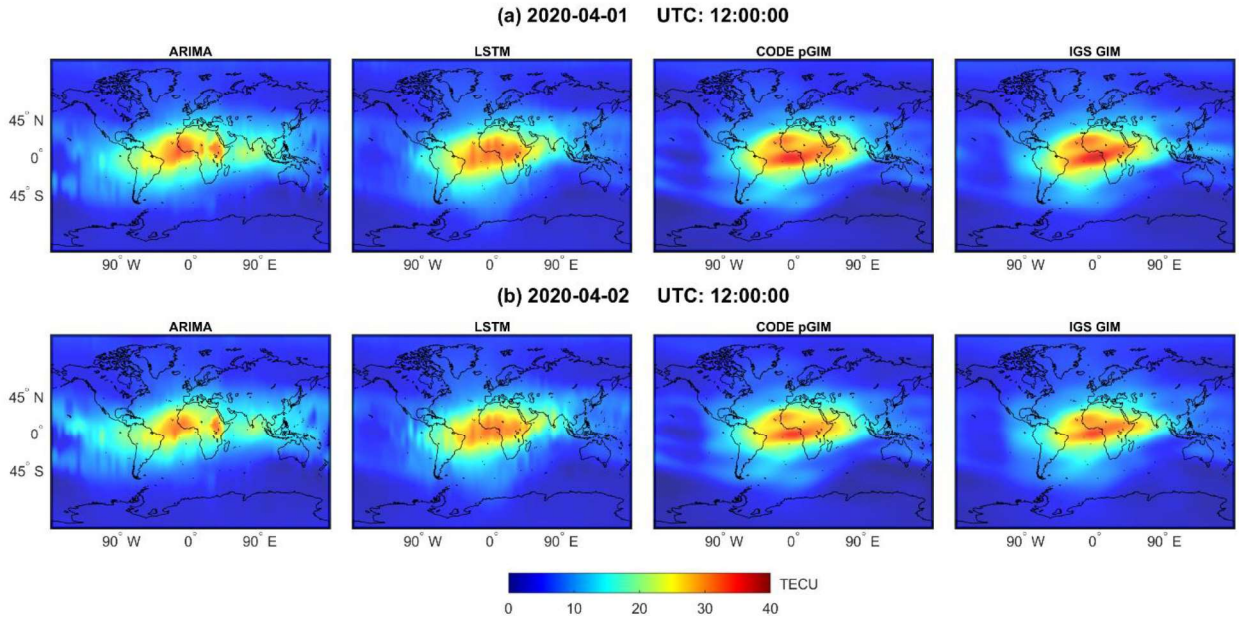

Figure 3: Global VTEC maps of ARIMA, LSTM, CODE pGIM, and IGS GIM at 12:00 UTC on April 1-2, 2020 (a) April 1, 2020 (b) April 2, 2020.

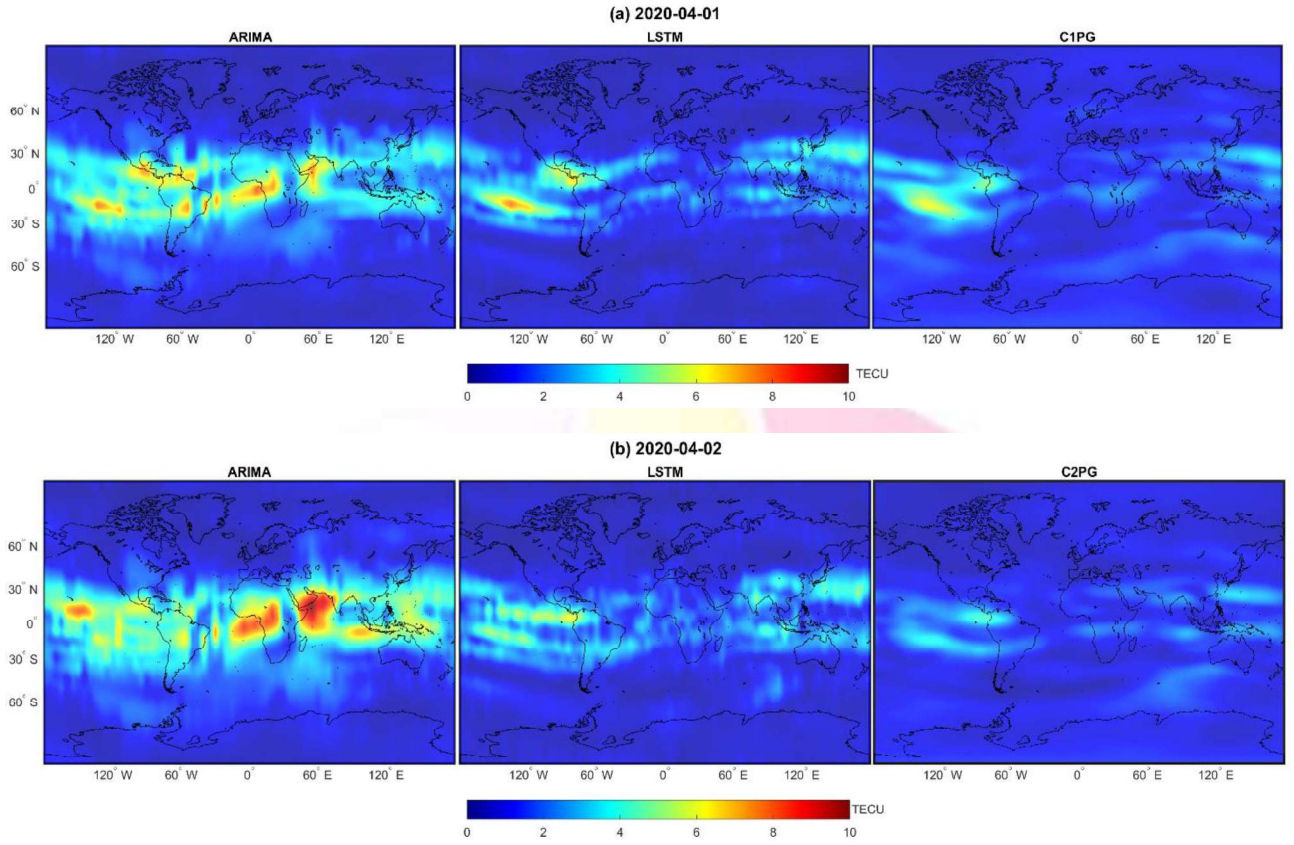

Figure 4: Daily RMS values of the differences between predicted GIMs and final IGS GIMs (a) April 1, 2020 (b) April 2, 2020.

Table 2 presents the bias and RMS values (unit: TECU) of the differences between predicted GIMs and final IGS GIMs on April 1-2, 2020. The values here are calculated for the differences in all grids for one day. RMS values showed that CODE pGIMs more consistent with final IGS GIMs than proposed methods both on April 1 and 2. The LSTM method had a lower accuracy of 5%-22% and the ARIMA method 37%-55% according to CODE pGIMs.

Table 2: Bias and RMS values of ARIMA, LSTM, and CODE pGIMs

Days	ARIMA		LSTM		C1PG - C2PG	
	BIAS	RMS	BIAS	RMS	BIAS	RMS
April 1	-0.58	2.54	-0.14	1.68	0.48	1.60
April 2	-0.84	2.94	-0.27	1.73	0.29	1.35

4. Conclusion

In this study, we tested the prediction capability of ARIMA and LSTM methods in producing predicted GIMs. The forecasting performance of proposed methods on the first day was found to be more accurate than the second day. We showed that LSTM is more successful than ARIMA for forecasting ionospheric VTECs, but CODE pGIMs is more accurate than the proposed models. Here, we have seen the capabilities and abilities of the AI-based models in forecasting the VTEC time series. We showed from our first results that deep learning methods provide more accurate forecast VTEC data. Future work aims to achieve better results than pGIMs of IGS IAACs (CODE, ESA, UPC, IGS combined) by changing the hyperparameters of the LSTM (e.g. increasing the number of hidden layers or iterations, using long-term training data) or using modified versions of LSTM (e.g. Bi-LSTM). In particular, we foresee that the multivariate approach will further improve the results of the proposed methods.

Acknowledgment

The author is thankful to the IGS and CODE for providing the GIMs, and OmniWeb NASA for providing the space weather indices.

5. References

Athieno, R., Jayachandran, P. T., Themens, D. R. (2017). A neural network-based foF2 model for a single station in the polar cap. Radio Science, 52(6), 784-796.

Box, G., Jenkings, G. (1970). Time Series Analysis: Forecasting and Control, Holden Day, San Francisco, USA.

Brunini, C., Meza, A., Azpilicueta, F., Van Zele, M. A., Gende, M., Díaz, A. (2004). A new ionosphere monitoring technology based on GPS. Astrophysics and Space Science, 290(3-4), 415-429.

Fedrizzi, M., de Paula, E. R., Kantor, I. J., Langley, R. B., Santos, M. C., Komjathy, A. (2002). Mapping the low-latitude ionosphere with GPS. GPS WORLD, 13(2), 41-47.

Fuller, W. A. (2009). Introduction to statistical time series (Vol. 428). John Wiley Sons.

Hargreaves, J. K. (1992). The solar-terrestrial environment: an introduction to geospace-the science of the terrestrial upper atmosphere, ionosphere, and magnetosphere. Cambridge university press.

Hernández-Pajares, M., Juan, J. M., Sanz, J., Aragón-Àngel, À., García-Rigo, A., Salazar, D., Escudero, M. (2011). The ionosphere: effects, GPS modeling and the benefits for space geodetic techniques. Journal of Geodesy, 85(12), 887-907.

Hochreiter, S., & Schmidhuber, J. (1997). Long short-term memory. Neural computation, 9(8), 1735-1780.

Ho, C. M., Mannucci, A. J., Lindqwister, U. J., Pi, X., Tsurutani, B. T. (1996). Global ionosphere perturbations monitored by the worldwide GPS network. Geophysical Research Letters, 23(22), 3219-3222.

Ivanov, V. B., Gefan, G. D., Gorbachev, O. A. (2011). Global empirical modelling of the total electron content of the ionosphere for satellite radio navigation systems. Journal of Atmospheric and Solar-Terrestrial Physics, 73(13), 1703-1707.

Jakowski, N., Mayer, C., Hoque, M. M., Wilken, V. (2011). Total electron content models and their use in ionosphere monitoring. Radio Science, 46(06), 1-11.

Kaselimi, M., Voulodimos, A., Doulamis, N., Doulamis, A., Delikaraoglou, D. (2020). A Causal Long Short-Term Memory Sequence to Sequence Model for TEC Prediction Using GNSS Observations. Remote Sensing, 12(9), 1354.

Klobuchar, J. A. (1987). Ionospheric time-delay algorithm for single-frequency GPS users. IEEE Transactions on aerospace and electronic systems, (3), 325-331.

Li, W., Zhao, D., He, C., Hu, A., Zhang, K. (2020). Advanced Machine Learning Optimized by The Genetic Algorithm in Ionospheric Models Using Long-Term Multi-Instrument Observations. Remote Sensing, 12(5), 866.

Mannucci, A. J., Wilson, B. D., Yuan, D. N., Ho, C. H., Lindqwister, U. J., Runge, T. F. (1998). A global mapping technique for GPS-derived ionospheric total electron content measurements. Radio science, 33(3), 565-582.

McKinnell, L. A., Poole, A. W. (2004). Predicting the ionospheric F layer using neural networks. Journal of Geophysical Research: Space Physics, 109(A8).

Pedregosa, F., Varoquaux, G., Gramfort, A., Michel, V., Thirion, B., Grisel, O., ... Vanderplas, J. (2011). Scikit-learn: Machine learning in Python. the Journal of machine Learning research, 12, 2825-2830.

Perez, R. O. (2019). Using TensorFlow-based Neural Network to estimate GNSS single frequency ionospheric delay (IONONet). Advances in Space Research, 63(5), 1607-1618.

Reddybattula, K. D., Panda, S. K., Ansari, K., Peddi, V. S. R. (2019). Analysis of ionospheric TEC from GPS, GIM and global ionosphere models during moderate, strong, and extreme geomagnetic storms over Indian region. Acta Astronautica, 161, 283-292.

Ruwali, A., Kumar, A. S., Prakash, K. B., Sivavaraprasad, G., Ratnam, D. V. (2020). Implementation of Hybrid Deep Learning Model (LSTM-CNN) for Ionospheric TEC Forecasting Using GPS Data. IEEE Geoscience and Remote Sensing Letters. DOI: 10.1109/LGRS.2020.2992633

Sai Gowtam, V., Tulasi Ram, S. (2017). An Artificial Neural Network-Based Ionospheric Model to Predict NmF2 and hmF2 Using Long-Term Data Set of FORMOSAT-3/COSMIC Radio Occultation Observations: Preliminary Results. Journal of Geophysical Research: Space Physics, 122(11), 11-743.

Sharma, K., Dabas, R. S., Ravindran, S. (2012). Study of total electron content variations over equatorial and low latitude ionosphere during extreme solar minimum. Astrophysics and Space Science, 341(2), 277-286.

Srivani, I., Prasad, G. S. V., Ratnam, D. V. (2019). A deep learning-based approach to forecast ionospheric delays for GPS signals. IEEE Geoscience and Remote Sensing Letters, 16(8), 1180-1184.